Available online at www.sciencedirect.com
ScienceDirect
Polymer 48 (2007) 3601–3606
polymer
www.elsevier.com/locate/polymer

Polymer translocation through a nanopore in mesoscopic simulations

Yan-Dong He, Hu-Jun Qian, Zhong-Yuan Lu*, Ze-Sheng Li*

State Key Laboratory of Theoretical and Computational Chemistry, Institute of Theoretical Chemistry, Jilin University, Changchun 130023, China

Received 20 January 2007; received in revised form 28 March 2007; accepted 11 April 2007
Available online 18 April 2007

Abstract

Dissipative particle dynamics (DPD) simulations are carried out to study the translocation of a single polymer chain through a pore under fluid field. The influences of the field strength E, the chain length N, the solvent quality α_{sp}, and the pore size h on the translocation time are evaluated. The translocation time τ, which is defined as the time that the chain moves through the pore completely in the direction of the driving force, scales with the field strength E as $\tau \sim E^{-0.48\pm0.01}$. We find that the translocation time is proportional to the chain length, which is in agreement with the experimental results and theoretical predictions. Tracing the variation of the square radius of gyration, R_g^2, and the polymer configuration during translocation, we observe that the chain is elongated when it is passing through the pore, which manifests that the chain is not in equilibrium during the translocation process. We also find that the worse the solvent quality is, the less time it will take to translocate, no matter what the size of the pore is. If the size of the pore is enlarged, the translocation time will be shorter. The information we gain from this study may benefit to the DNA sequencing.

Keywords: Polymer translocation; Dissipative particle dynamics simulation; Nanopore

1. Introduction

The translocation of a polymer chain through narrow channels or pores under external fields is an essential mechanism for life processes and industrial phenomena. The motion of biomolecules across biological pores is ubiquitous in organisms, such as DNA and RNA translocation across nuclear pores, protein transporting through membrane channels, gene swapping through bacterial pili, and the injection of viral DNA into a host cell [1–3]. With the development of a variety of biotechnologies, this simple transportation behavior is also applied in rapid DNA sequencing, gene therapy, and delivery of drug molecules to their activation sites [4–8]. In industry, the separation and purification of synthetic or biological macromolecules, the recovery and separation of oil, the production of foods and medicine are all related to the translocation of polymer chains.

Therefore, the polymer translocation had attracted a large number of scientists, investigating its underlying physics via a variety of experiments [9–17], theories [18–29] and numerical simulations [30–39]. Although the actual biological (or industrial) system is complicated, a primitive model, including a polymer chain and an infinite planar wall with a small hole, is always used to understand the basic physics of translocation. Intuitively we can consider, when the polymer chain translocates through the small pore, a large entropic barrier will be set up due to the lost of the number of configurations, therefore an external driving force is requested to speed up the translocation. In order to achieve this, some methods had been applied, such as the electric fields [9,11], the ratchet mechanism [40], the chemical potential gradients [21], and the selective adsorption of the chain on one side of the membrane [19]. For example, Kasianowicz et al. [9], in an experiment, showed that an electric field can drive single-stranded DNA and RNA molecules through an ion channel in a lipid bilayer membrane. In recent experiment, Storm et al. [14] argued that fast DNA translocation through a solid-state nanopore is determined by a balance between the driving force and the hydrodynamic drag on the molecule.

* Corresponding authors.
E-mail addresses: luzhy@mail.jlu.edu.cn (Z.-Y. Lu), zeshengli@mail.jlu.edu.cn (Z.-S. Li).

0032-3861/$ - see front matter © 2007 Elsevier Ltd. All rights reserved.
doi:10.1016/j.polymer.2007.04.016

Inspired by the experiments, a number of theoretical studies of the translocation process had been conducted. Sung and Park [18] described equilibrium entropy of the polymer as a function of the position of the polymer across the nanopore and assumed constant chain diffusivity. Muthukumar [21] suggested a linear dependence between the translocation time and the chain length ($\tau \sim N$) under a strong field with classical nucleation theory. Recently, some researchers constructed various models with different dynamics simulation techniques to study the physics of this fundamental biological (and industrial) processes. Sometimes different results were obtained, because different models and interaction types between polymer chain and nanopore were adopted. For example, some methods were fulfilled by making the first monomer of the polymer chain immovable with artificial restriction at the beginning of the simulations. This may bias the actual physics of translocation.

In general, the translocation process includes three steps. First, the pore is filled with part of the chain (M segments) from the donor container, and the average translocation time is τ_1. During the second step, with average translocation time τ_2, $(N-M)$ segments are transferred from the donor to the recipient container. Here, N is the polymer chain length and M is the nanopore length ($M<N$). In the third step, M chain segments leave the pore and enter the recipient container with the average translocation time τ_3. The total translocation time is $\tau=\tau_1+\tau_2+\tau_3$ [37]. In most cases, N is much larger than M and τ_2 determines the total translocation time. Therefore, in this research, we select a minimum wall model with the thickness being comparable to the simulated bead size and analyze the effects of the field strength, the solvent quality, the chain length, and the pore size on the chain translocation dynamics. The bond force constant is selected such that the bead can interact with the nearest and the second nearest beads along the chain backbone. This results in a wormlike chain model. In Section 2, we briefly describe the model and the simulation method. In Section 3, using our approach we analyze the results and reasoning. Section 4 is a short conclusion.

2. Model and method

The dissipative particle dynamics (DPD) simulation method, which is well developed to describe fluid, is adopted here, because it allows larger integration time step owing to its soft potential. However, in DPD, the soft nature of the bead–bead interaction cannot prevent the penetration of simulated solvent or polymer beads into the wall. Thus we construct the wall model following Ref. [41], in which the wall is impenetrable by applying bounce back boundary condition. In the middle of the wall a pore is made allowing the translocation of the polymer chain. During the simulations, the positions of the wall particles do not change. Another thing should be mentioned is that we place the first polymer bead in the right side of the wall and the rest in the left side of the wall, instead of the first bead being fixed artificially during the simulation.

In DPD, the motion of particles is governed by Newton's equation of motion [42],

$$\frac{\mathrm{d}\vec{r}_i}{\mathrm{d}t}=\vec{v}_i,$$

$$\frac{\mathrm{d}\vec{v}_i}{\mathrm{d}t}=\vec{f}_i.$$

The force acting on a solvent bead is a sum of the conservative, the dissipative, the random, and the fluid field forces, i.e.,

$$\vec{f}_i=\sum_{j\neq i}\vec{F}_{ij}^{\mathrm{C}}+\vec{F}_{ij}^{\mathrm{D}}+\vec{F}_{ij}^{\mathrm{R}}+\vec{F}_{\mathrm{driving}}.$$

For a polymer bead, another spring force is needed. The different parts of the forces are given by:

$$\vec{F}_{ij}^{\mathrm{C}}=\begin{cases}a_{ij}(1-r_{ij})\hat{r}_{ij} & (r_{ij}<1)\\ 0 & (r_{ij}\geq 1)\end{cases},$$

$$\vec{F}_{ij}^{\mathrm{D}}=-\gamma\omega^{\mathrm{D}}(r_{ij})(\hat{r}_{ij}\cdot\vec{v}_{ij})\hat{r}_{ij},$$

$$\vec{F}_{ij}^{\mathrm{R}}=\sigma\omega^{\mathrm{R}}(r_{ij})\xi_{ij}\Delta t^{-1/2}\hat{r}_{ij},$$

$$\vec{F}_{\mathrm{driving}}=\text{constant},$$

$$\vec{F}_{\mathrm{spring}}=-k\vec{r}_{ij}.$$

The conservative force $\vec{F}_{ij}^{\mathrm{C}}$ is a soft repulsion acting along the line of bead centers, and a_{ij} is a maximum repulsion between particles i and j. $\vec{r}_{ij}=\vec{r}_i-\vec{r}_j$, $r_{ij}=|\vec{r}_{ij}|$, and $\hat{r}_{ij}=\vec{r}_{ij}/|\vec{r}_{ij}|$. ξ_{ij} is a random number with zero mean and unit variance, and is chosen independently for each interacting pair of particles at each time step Δt. ω^{D} and ω^{R} are two weight functions for the dissipative and random forces, respectively. $\omega^{\mathrm{D}}(r)=[\omega^{\mathrm{R}}(r)]^2$ and $\sigma^2=2\gamma k_{\mathrm{B}}T$, so that the system samples a canonical ensemble [43]. The polymer chain is constructed by connecting the neighboring beads together with the spring force $\vec{F}_{\mathrm{spring}}$. The spring constant $k=100$ such that the bead can interact with the nearest and the second nearest beads along the chain backbone. This results in the three-body correlation between the nearest consecutive beads and further results in a wormlike chain model. In the simulations $r_{\mathrm{c}}=1$, $m=1$, and $k_{\mathrm{B}}T=1$, setting the units of the system. The densities of the solution and the wall are all kept equal to 3. The wall thickness is 1 and the pore size (h) is initially set to be 1. In order to study the effect of the pore size, h can be changed to other values. The simulation box, which is a primitive model, is two-dimensional with size 120×120 or 300×100 depending on the simulated chain length. The polymer is initially configured randomly with the requirement that only the first bead is on the right side of the wall and the rest is on the left side. It should be noted that not all simulation runs are successful translocations. We have conducted a series of the runs with different initial chain configurations and consider only the average translocation time τ over all successful runs.

3. Results and discussion

In the beginning of the simulations, the first monomer is put in the recipient box near to the pore, as sketched in Fig. 1. Without external field, the first monomer will be pull back to the donor box in a very short time simulation. Therefore, to facilitate the chain translocation, an extra directional field is needed just like in experiments. We have adopted here the simplest field, i.e., adding constant and homogeneous force on the particles. Only by doing this, the chain can overcome the large entropic barrier due to the loss of the number of the configurations during polymer translocation in our simulations. As shown in Fig. 2(a), at weak field strength (i.e., the driving force), the translocation time τ decreases rapidly with increasing field strength, whereas τ tends to reach a plateau for strong fields. Increasing the field strength effectively enhances the velocities of the particles and reduces the translocation time. However, due to the existence of the pore, the polymer velocity is not dominated by the strength of the field, especially for large E. This phenomenon is similar to the result of Matysiak et al. [44] which is attributed to the change in translocation mechanism from barrier crossing to downhill. In Fig. 2(b), we fit the translocation time against the external field and find the scaling relation $\tau \sim E^{-0.48\pm0.01}$. Such a dependence of the translocation time on the external field is weaker than the cases in Refs. [30,36]. It may be ascribed that we have adopted the soft potentials and bounce back boundary condition.

We have also considered the influence of the chain length on the translocation time in the condition with different pore sizes. Fig. 3 shows the dependence of τ on N for three different pore sizes. We find that τ appears to increase almost linearly with N, which is in agreement with the experiments [9,13] that found the channel blockade lifetime was proportional to polymer length. By increasing the size of the pore, the polymer chain is easier, or faster, to be translocated through the pore, in the case of same chain length. This is because that the larger the pore is, the less the confinement acting on the polymer chain from the pore is, which surely benefits to the mobility of the polymer. Although Storm et al. [15] found

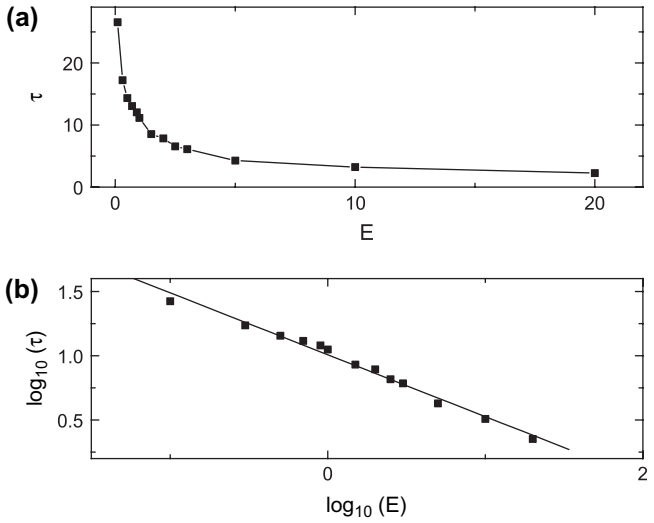

Fig. 2. (a) shows the translocation time τ as a function of field strength E for $N = 100$; (b) is the double log plot. The slope of the fitting line is 0.48 ± 0.01.

an exponent of 1.27 in the solid-state nanopore experiments in three dimensions, the present study supports the results of the experiments on *α-hemolysin* [9,13] and the theory of Muthukumar [21]. Such a scaling is different from that found in the Langevin dynamics simulations [36], which show $\tau \sim N^{2\nu}$ for relatively short chains to $\tau \sim N^{1+\nu}$ for longer chains in the case of intermediate friction coefficient, where ν is the Flory exponent. It may be because that in our model, the friction is small owing to the adopted soft potential. Also, the forced translocation times are shown to strongly depend on the method by which the force is applied [32].

To study translocation dynamics in detail, we calculate the square radius of gyration R_g^2 during the translocation for different polymer chain lengths. Because the direction of the field is along the X direction, $R_{g,x}^2$ is dominant to R_g^2. For different chain lengths N from 10 to 100, the variations of R_g^2 are shown in Fig. 4. Clearly the chain has large configuration change during the translocation. First, R_g^2 decreases before the polymer translocating through the pore, which is attributed to the

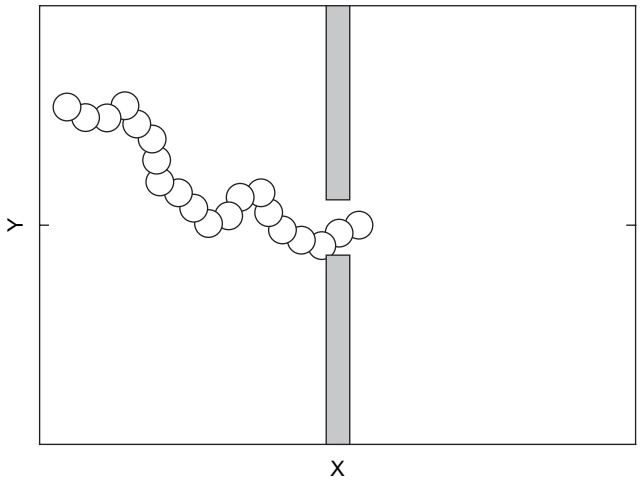

Fig. 1. The sketch of the model.

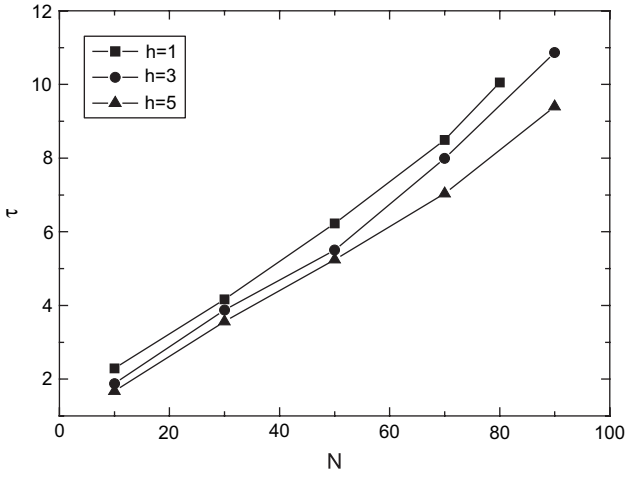

Fig. 3. Average translocation time as a function of chain length for pore size $h = 1$, 3, and 5.

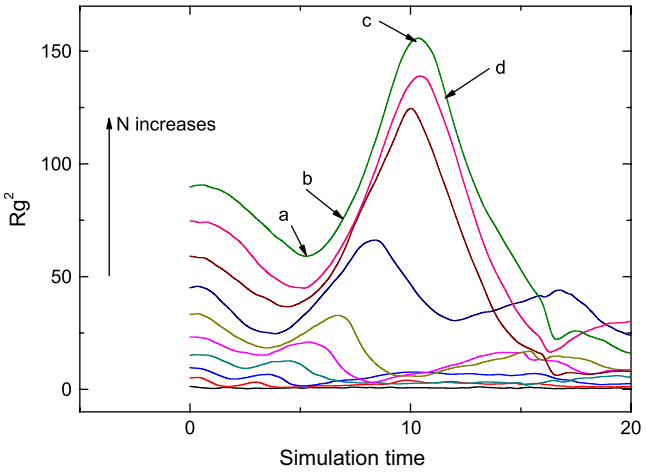

Fig. 4. The variation of the square radius of gyration R_g^2 of polymer during the translocation for $N = 10$ to $N = 100$.

constant compression force from external field on the polymer chain. When more and more beads start to translocate, R_g^2 decreases to its minimum, as shown by (a) in Fig. 4. Afterwards, R_g^2 increases monotonically until reaches to the maximum, as shown by (c) in Fig. 4. This implies that the polymer is extended during translocation, and the part of the chain is stretched by the field in the recipient box. It should be noted that the time reaching the maximum of R_g^2 does not correspond to the moment that the polymer is translocated through the pore completely. After reaching the maximum of R_g^2, most of the polymer beads have been translocated through the pore, and the configuration relaxation causes R_g^2 to decrease again, corresponding to (d) in Fig. 4. From the variation of R_g^2, we can conclude that the translocation of polymer is not in an equilibrium state during the translocation process and the polymer chain is elongated. This result is in agreement with that of Luo et al. [35] who had demonstrated that the polymer remains in nonequilibrium during translocation using Monte Carlo simulations. In Fig. 5, we show the instantaneous configuration snapshots of the chain with $N = 100$ at different times corresponding to the arrows in Fig. 4. The translocation time is estimated as 11.162 in reduced unit for this system.

In our simulations, we also consider the effect of the solvent quality on the polymer translocation. When the quality of the solvent is changed from good to poor, the effective attractive interactions between monomers can cause the polymer configuration transition from a swollen to a compact state [45–47]. This configuration transition relates to the entropy loss, thus may further influence the polymer translocation through a pore. By fixing the interactions between polymer and polymer, and between solvent and solvent, we change the interaction between polymer and solvent from 75 to 5 to manifest the change from the bad to the good solvent. By simulating this series of systems, we obtain the dependence of polymer translocation time on the solvent quality, which is shown in Fig. 6(a) for $N = 80$, 90, and 100. From the figure we can see that the worse the solvent quality is, the faster the polymer translocates through the pore. This is mainly

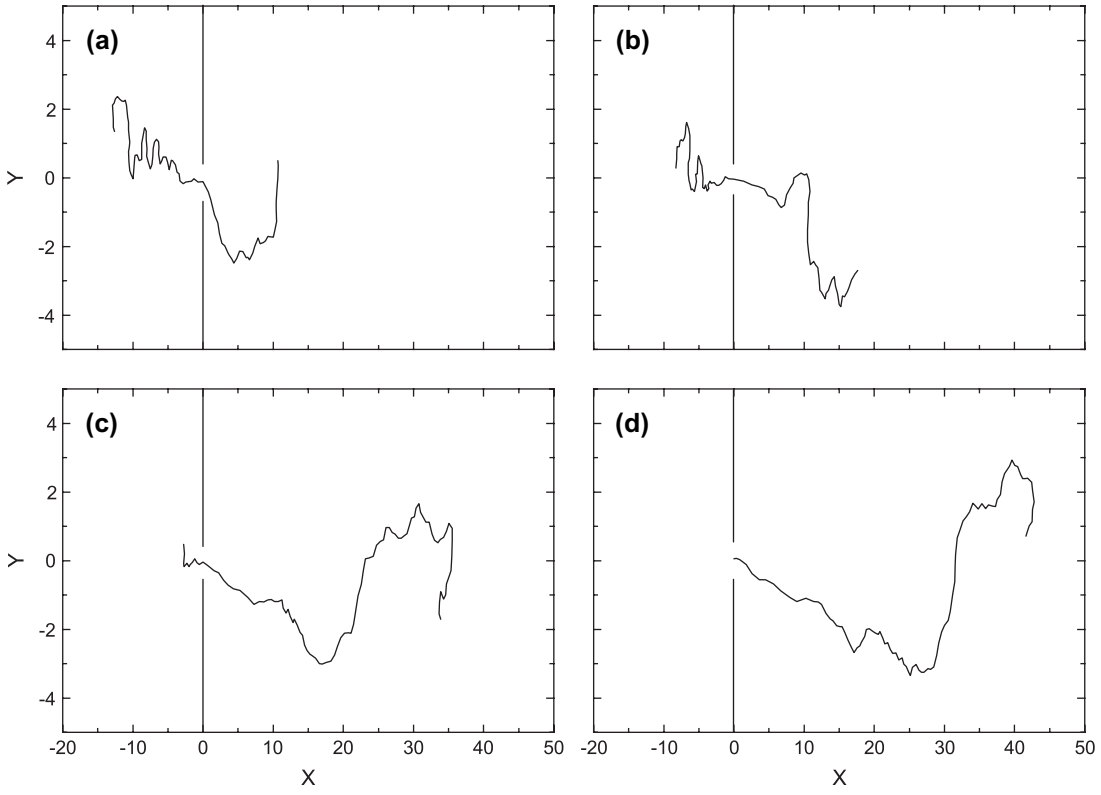

Fig. 5. Configurations for the chain with $N = 100$ during translocation: (a) 33 beads are translocated at $t = 5.146$ and the configuration corresponds to (a) in Fig. 4; (b) 50 beads are translocated at $t = 6.986$ and the configuration corresponds to (b) in Fig. 4; (c) 87 beads are translocated at $t = 10.248$ and the configuration corresponds to (c) in Fig. 4; (d) all of the beads are translocated at $t = 11.162$ and the configuration corresponds to (d) in Fig. 4.

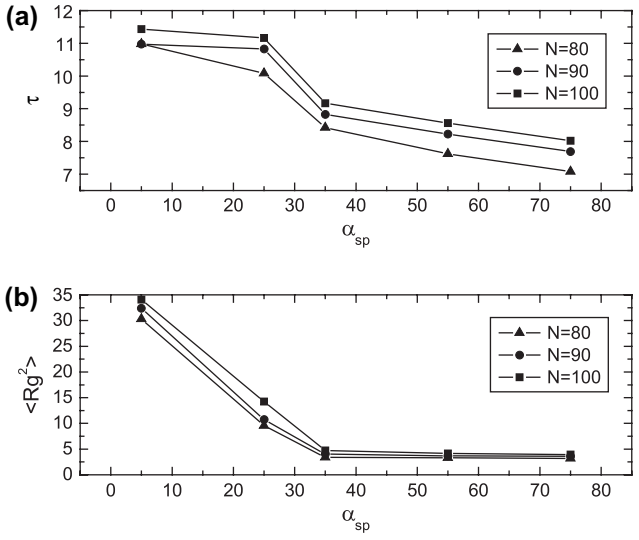

Fig. 6. (a) Average translocation time as a function of the solvent quality α_{sp}. The field strength E is 1.0 and the pore size h is 1.0. The squares, circles and triangles represent for $N = 80$, 90, and 100, respectively. (b) The mean square radius of gyration changes with the solvent quality α_{sp}.

attributed to the entropy decrease by decreasing the solvent quality in our model. The mean square radius of gyration is calculated with different solvent quality to see what is the chain size variation with increasing α_{sp}. The results, which are shown in Fig. 6(b), demonstrate that the mean square radius of gyration of the polymer chain decreases with increasing α_{sp}. Specifically, the size of the chain decreases rapidly when α_{sp} increases from 5 to 35, whereas it does not change much when α_{sp} increases from 35 to 75. The rapid decrease of the radius of gyration when the solvent quality changes from good to poor may correspond to a coil to globule transition. Apparently, the polymer chain in good solvent condition has a larger entropy change when translocating through the pore as compared to that in bad solvent condition. The effects of solvent quality on the translocation time are reduced with increasing pore sizes, which are shown in Fig. 7. The

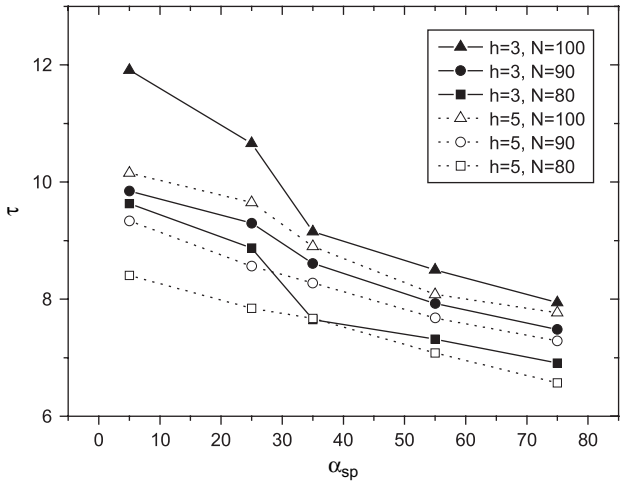

Fig. 7. Average translocation time as a function of the solvent quality α_{sp} for different pore sizes. The solid lines are for $h = 3$ and dotted lines for $h = 5$. The squares, circles and triangles represent for $N = 80$, 90, and 100, respectively.

confinement due to the pore is reduced at larger pore sizes, therefore the entropy change is not as much as that in the case of $h = 1$. The free energy barrier induced by solvent quality is crucial for controlling the translocation time, thus may provide a hint to the rapid DNA sequencing in experiments.

4. Conclusion

We have investigated the dynamics of polymer translocation through a nanopore under an external homogeneous fluid field in two dimensions with DPD simulations. With large bond force constant, we are trying to model the wormlike chain. The translocation time decreases rapidly with increasing the field strength in the small field strength region, in which the field strength dominates the translocation. But in the strong field region, the influence of the field strength is not so drastic, which gradually reaches to a plateau. The larger the pore is, the weaker the repulsive interaction is, thus benefits to the faster translocation of the polymer. The translocation time increases almost linearly with increasing the polymer chain length. Moreover, the translocation is affected by the solvent quality. When the polymer is in the bad solvent condition, it is easier to translocate under the field. By following the changes of the mean square radius of gyration during the translocation, we find that the polymer is largely extended in the process.

References

[1] Alberts B, Bray D. Molecular biology of the cell. New York: Garland Publishing; 1994.
[2] Darnell J, Lodish H, Baltimore D. Molecular cell biology. New York: Scientific American Books; 1995.
[3] Miller RV. Sci Am 1998;66:278.
[4] Han J, Turner SW, Craighead HG. Phys Rev Lett 1999;83:1688.
[5] Turner SWP, Cabodi M, Craighead HG. Phys Rev Lett 2002;88:128103.
[6] Chang DC. Guide to electroporation and electrofusion. New York: Academic Press; 1992.
[7] Han J, Graighead HG. Science 2000;288:1026.
[8] Hanss B, Leal-pinto E, Bruggeman LA, Copeland TD, Klotman PE. Proc Natl Acad Sci USA 1998;95:1921.
[9] Kasianowicz JJ, Brandin E, Branton D, Deamer DW. Proc Natl Acad Sci USA 1996;93:13770.
[10] Aktson M, Branton D, Kasianowicz JJ, Brandin E, Deamer DW. Biophys J 1999;77:3227.
[11] Meller A, Nivon L, Brandin E, Golovchenko JA, Branton D. Proc Natl Acad Sci USA 2000;97:1079.
[12] Henrickson SE, Misakian M, Robertson B, Kasianowicz JJ. Phys Rev Lett 2000;85:3057.
[13] Meller A, Nivon L, Branton D. Phys Rev Lett 2001;86:3435.
[14] Storm AJ, Chen JH, Ling XS, Zandbergen HW, Dekker C. Nat Mater 2003;2:537.
[15] Storm AJ, Storm C, Chen JH, Zandbergen H, Joanny JF, Dekker C. Nano Lett 2005;5:1193.
[16] Kwan KS, Subramaniam CNP, Ward TC. Polymer 2003;44:3061.
[17] Kwan KS, Subramaniam CNP, Ward TC. Polymer 2003;44:3071.
[18] Sung W, Park PJ. Phys Rev Lett 1996;77:783.
[19] Park PJ, Sung W. J Chem Phys 1998;108:3013.
[20] Di Marzio EA, Mandell AJ. J Chem Phys 1997;107:5510.
[21] Muthukumar M. J Chem Phys 1999;111:10371.
[22] Lubensky DK, Nelson DR. Biophys J 1999;77:1824.
[23] Muthukumar M. Phys Rev Lett 2001;86:3188.

[24] Ambjörnsson T, Apell SP, Konkoli Z, Di marzio EA, Kasianowicz JJ. J Chem Phys 2002;117:4063.
[25] Muthukumar M. J Chem Phys 2003;118:5174.
[26] Slonkina E, Kolomeisky AB. J Chem Phys 2003;118:7112.
[27] Matsuyama A. J Chem Phys 2004;121:8098.
[28] Ambjörnsson T, Lomholt MA, Metzler R. J Phys Condens Matter 2005;17:S3945.
[29] Luo KF, Ala-Nissila T, Ying SC. J Chem Phys 2006;124:034714.
[30] Chuang J, Kantor Y, Kardar M. Phys Rev E 2001;65:011802.
[31] Tian P, Smith GD. J Chem Phys 2003;119:11475.
[32] Kantor Y, Kardar M. Phys Rev E 2004;69:021806.
[33] Ali I, Yeomans JM. J Chem Phys 2005;123:234903.
[34] Huopaniemi I, Luo KF, Ala-Nissila T, Ying SC. Phys Rev E 2006;19:10.
[35] Luo KF, Huopaniemi I, Ala-Nissila T, Ying SC. J Chem Phys 2006; 124:114704.
[36] Huopaniemi I, Luo KF, Ala-Nissila T, Ying SC. J Chem Phys 2006; 125:124901.
[37] Xie YJ, Yang HY, Yu HT, Shi QW, Wang XP, Chen J. J Chem Phys 2006;124:174906.
[38] Lansac Y, Maiti PK, Glaser MA. Polymer 2004;45:3099.
[39] Luo MB. Polymer 2005;46:5730.
[40] Simon SM, Peskin CS, Oster GF. Proc Natl Acad Sci USA 1992; 89:3770.
[41] Pivkin IV, Karniadakis GE. J Comput Phys 2005;207:114.
[42] Groot RD, Warren PB. J Chem Phys 1997;107:4423.
[43] Español P, Warren PB. Europhys Lett 1995;30:191.
[44] Matysiak S, Montesi A, Pasquali M, Kolomeisky AB, Clementi C. Phys Rev Lett 2006;96:118103.
[45] Doi M, Edwards SF. The theory of polymer dynamics. Oxford: Clarendon Press; 1986.
[46] de Gennes PG. Scaling concepts in polymer physics. New York: Cornell University Press; 1979.
[47] Kikuchi N, Ryder JF, Pooley CM, Yeomans JM. Phys Rev E 2005; 71:061804.